

Are your MRI contrast agents cost-effective?

Learn more about generic Gadolinium-Based Contrast Agents.



FRESENIUS  
KABI

caring for life

**AJNR**

**Longitudinal MRI Evaluation of Brain Development in Fetuses with Congenital Diaphragmatic Hernia around the Time of Fetal Endotracheal Occlusion**

D. Eman, M. Aertsen, L. Van der Veeken, L. Fidon, P. Patkee, V. Kyriakopoulou, L. De Catte, F. Russo, P. Demaerel, T. Vercauteren, M. Rutherford and J. Deprest

This information is current as of April 18, 2024.

*AJNR Am J Neuroradiol* published online 19 January 2023  
<http://www.ajnr.org/content/early/2023/01/19/ajnr.A7760>

# Longitudinal MRI Evaluation of Brain Development in Fetuses with Congenital Diaphragmatic Hernia around the Time of Fetal Endotracheal Occlusion

 D. Emam,  M. Aertsen,  L. Van der Veeken,  L. Fidon,  P. Patkee,  V. Kyriakopoulou,  L. De Catte, F. Russo,  P. Demaerel,  T. Vercauteren,  M. Rutherford, and  J. Deprest



## ABSTRACT

**BACKGROUND AND PURPOSE:** Congenital diaphragmatic hernia is associated with high mortality and morbidity, including evidence suggesting neurodevelopmental comorbidities after birth. The aim of this study was to document longitudinal changes in brain biometry and the cortical folding pattern in fetuses with congenital diaphragmatic hernia compared with healthy fetuses.

**MATERIALS AND METHODS:** This is a retrospective cohort study including fetuses with isolated congenital diaphragmatic hernia between January 2007 and May 2019, with at least 2 MR imaging examinations. For controls, we used images from fetuses who underwent MR imaging for an unrelated condition that did not compromise fetal brain development and fetuses from healthy pregnant women. Biometric measurements and 3D segmentations of brain structures were used as well as qualitative and quantitative grading of the supratentorial brain. Brain development was correlated with disease-severity markers.

**RESULTS:** Forty-two fetuses were included, with a mean gestational age at first MR imaging of 28.0 (SD, 2.1) weeks and 33.2 (SD, 1.3) weeks at the second imaging. The mean gestational age in controls was 30.7 (SD, 4.2) weeks. At 28 weeks, fetuses with congenital diaphragmatic hernia had abnormal qualitative and quantitative maturation, more extra-axial fluid, and larger total skull volume. By 33 weeks, qualitative grading scores were still abnormal, but quantitative scoring was in the normal range. In contrast, the extra-axial fluid volume remained abnormal with increased ventricular volume. Normal brain parenchymal volumes were found.

**CONCLUSIONS:** Brain development in fetuses with congenital diaphragmatic hernia around 28 weeks appears to be delayed. This feature is less prominent at 33 weeks. At this stage, there was also an increase in ventricular and extra-axial space volume.

**ABBREVIATIONS:** CDH = congenital diaphragmatic hernia; FETO = fetal endotracheal occlusion; GA = gestational age; SRR = super-resolution reconstruction; TFLV = total fetal lung volume

Congenital diaphragmatic hernia (CDH) is a severe birth defect, occurring in approximately 1 in 3000 live-born neonates.<sup>1</sup> Despite neonatal treatment, the disease is associated with

high mortality, and survivors often have short- and long-term morbidities.<sup>1</sup> These include respiratory, gastrointestinal, and neurologic impairments.<sup>2</sup> Neurodevelopmental delays as well as behavioral difficulties have been linked to CDH in the past, and certain risk factors have been suggested, including gestational age at birth, disease severity, associated anomalies, the requirement for extracorporeal membrane oxygenation, and long stays in the neonatal intensive care unit.<sup>2-7</sup>

In infants with CDH, imaging studies have demonstrated several abnormalities, including increased extra-axial space, delayed sulcation, and white matter injury, but the exact mechanisms

Received April 28, 2022; accepted after revision December 10.


From the Department of Development and Regeneration (D.E., L.V.d.v., L.D.C., F.R., J.D.), Cluster Woman and Child, Group Biomedical Sciences, KU Leuven University of Leuven, Leuven, Belgium; Department Obstetrics and Gynaecology (D.E., L.F.), Faculty of Medicine, Tanta University, Tanta, Egypt; Department of Imaging and Pathology (M.A., P.D.), Clinical Department of Radiology, University Hospitals, KU Leuven, Leuven, Belgium; Clinical Department Obstetrics and Gynaecology (L.V.d.v., L.D.C., F.R., J.D.), University Hospitals Leuven, Leuven, Belgium; Centre for the Developing Brain (P.P., V.K., M.R., J.D.), Division of Imaging Sciences and Biomedical Engineering, Perinatal Imaging and Health and School of Biomedical Engineering and Imaging Sciences (L.F., T.V., J.D.), King's College London, King's Health Partners, St. Thomas' Hospital, London, UK; and Institute for Women's Health (J.D.), University College London, London, UK.

D. Emam and M. Aertsen contributed equally to this work.

D.E. is funded by the Egyptian Educational Scholarship from the Ministry of Higher Education and Scientific Research, Egypt. L.V.d.v. is funded by the Erasmus+ Program of the European Union (framework agreement no. 2013-0040). J.D. and T.V. receive support from the Wellcome Trust (WT101957) and the Engineering and Physical Sciences Research Council (NS/A000027/1). J.D. receives support from the Great Ormond Street Hospital Charity Fund. To support L.F. and T.V., this project has received funding from the European Union's Horizon 2020 research and innovation program under the Marie Skłodowska-Curie grant agreement No 765148.

This publication reflects the views only of the authors, and the Commission cannot be held responsible for any use that may be made of the information contained therein.

Please address correspondence to Michael Aertsen, MD, Department of Radiology, University Hospitals Leuven, Herestraat 49, 3000 Leuven, Belgium; e-mail: Michael.aertsen@uzleuven.be

 Indicates open access to non-subscribers at [www.ajnr.org](http://www.ajnr.org)

 Indicates article with online supplemental data.

<http://dx.doi.org/10.3174/ajnr.A7760>

remain unclear.<sup>8</sup> As for other congenital malformations with an increased risk for neurodevelopmental abnormalities, parents may ask whether these are already present at the time of prenatal diagnosis or are more likely to be postnatally acquired. This issue will become even more important with the advent of effective fetal therapy,<sup>9-11</sup> which treats fetuses with the more severe forms of CDH. Those parents and physicians likewise will want to understand whether brain development in CDH is already altered prenatally and, when present, if this would be severity-dependent.<sup>12</sup> Currently, there are limited data on in utero brain development in fetuses with CDH.<sup>8,12,13</sup> Radhakrishnan et al<sup>12</sup> described enlargement of the extra-axial space and congestion of the venous sinuses in the third trimester. A further study reported a correlation between cerebellar and vermian dimensions and the severity of lung hypoplasia (evidenced by lower fetal lung volume). Recently, we reported, on the basis of sonography, changes in cerebellar growth, in particular after 32 weeks' gestation. We also correlated these to disease severity.<sup>14</sup> The objective in the present study was to use MR imaging data to document cortical folding as well as the dimensions and volume of given brain structures in comparison with findings in healthy fetuses, again, in particular, late in gestation.

## MATERIALS AND METHODS

This retrospective cohort study included all consecutive fetuses diagnosed with isolated CDH at the University Hospitals Leuven, Belgium, between January 2007 and May 2019 ( $n = 283$ ) and for whom at least 2 MR imaging examinations were available ( $n = 48$  fetuses). Isolated CDH was defined as the presence of normal findings on prenatal genetic testing (conventional karyotyping or comparative genome-wide hybridization array analysis<sup>15</sup>) and the absence of a major structural anomaly. Fetuses with poor-quality brain images due to motion artifacts were excluded ( $n = 6$ ). For controls, we used images from fetuses that underwent MR imaging for an unrelated condition, which was presumed not to involve brain development, assessed between 20 and 37 weeks' gestational age (GA) ( $n = 26$ ). The precise indications for MR imaging assessment are provided in the Online Supplemental Data. All brain examinations were reported as showing normal appearances for GA, and no abnormal neurodevelopmental outcome was reported after birth. We added to this control cohort additional fetal images ( $n = 30$ ) obtained by our collaborators from King's College London (Robert Steiner MR Imaging Unit in Hammersmith Hospital, London, UK) between November 2007 and May 2013 in healthy pregnant women who had normal neurodevelopmental follow-up. These data were included in a previous study.<sup>16</sup> Selected patients were chosen to be equally distributed across the same GA period.

### MR Imaging Examination

At the University Hospitals Leuven, MR imaging was performed as part of standard clinical care using a 1.5T system (Aera; Siemens). Two small body coils were placed adjacent to each other over the mother. The mother was positioned in the supine or left lateral decubitus position. Before September 2015, maternal sedation (flunitrazepam, 0.5 mg taken orally 20–30 minutes before the examination) was used when the GA was <30 weeks,

a practice that was abandoned.<sup>17,18</sup> The protocol includes T2-weighted HASTE sequences, obtained in 3 orthogonal planes relative to the fetal head (coronal, axial, and sagittal). Scanning parameters are reported elsewhere.<sup>19</sup> In addition, T2-weighted HASTE sequences, obtained in 3 orthogonal planes relative to the fetal body (coronal, axial, and sagittal) were performed. Scanning parameters were TE = 90 ms; TR = 1000 ms; section thickness = 3.0–4.0 mm; absence of an intersection gap; FOV = 300 × 300–380 × 380 mm. During the study period, the scanner received several software updates that had no influence on the image quality of T2-weighted sequences. However, additional sequences were added to the routine protocol (eg, T2\*-weighted sequences and diffusion-weighted imaging), but these are not relevant to this study. Parameters from the MR imaging examination in controls scanned at the Robert Steiner MR Imaging Unit in Hammersmith Hospital, London, UK, were similar and can be found in Kyriakopoulou et al.<sup>16</sup> These examinations were performed using a 1.5T MR imaging system (Achieva; Philips Healthcare) with a 32-channel cardiac array coil. The mother was positioned in a left lateral tilt, and no sedation was used. The images used for this study included T2-weighted images in transverse, sagittal, and coronal planes.

### Assessment of Brain Development and Severity of Pulmonary Hypoplasia

Biometric measurements were obtained on standard T2-weighted images and included brain and skull biparietal diameter and fronto-occipital diameter, atrial width, and transverse cerebellar diameter (Online Supplemental Data).<sup>17</sup> Head circumference and extra-axial space percentiles were calculated according to Kyriakopoulou et al.<sup>16</sup> Fetal cortical development was scored using the grading system described by Pistorius et al<sup>20</sup> and measured following Egaña-Ugrinovic et al.<sup>21</sup> We earlier demonstrated that scoring has a good interobserver reproducibility.<sup>22</sup> All measurements were performed by D.E. (with limited experience in fetal MR imaging) under direct supervision of M.A. (with >5 years' experience in fetal MR imaging with >2000 fetal MR imaging examinations) after training in scoring the fetal brain on MR imaging with the qualitative and quantitative grading system in 15 cases. The following brain regions were scored subjectively: frontal, parietal, temporal, mesial, insular, and occipital cortex.<sup>20</sup> Selected primary sulci and gyri were graded and/or measured, including the parieto-occipital fissure; the central, calcarine, superior temporal, cingulate sulcus; and, for the opercularization, the Sylvian fissure.<sup>20,21</sup> In addition to the Sylvian fissure depth, which reflects the distance between the inner part of the skull and the insular cortex, the insular depth was also measured, ie, the distance from the midline to the insular cortex.<sup>22</sup> The sum of all the graded fissures provides a total grading score for each hemisphere and the whole brain.<sup>22</sup>

3D super-resolution reconstruction (SRR) volumes were created from the standard T2-weighted 2D stacks displaying the fetal brain, using NiftyMIC (<https://github.com/gift-surg/NiftyMIC>), a publicly available and state-of-the-art SRR algorithm.<sup>23</sup> The SRR volumes were automatically segmented for white matter, the ventricular system (lateral ventricles, third ventricle, fourth

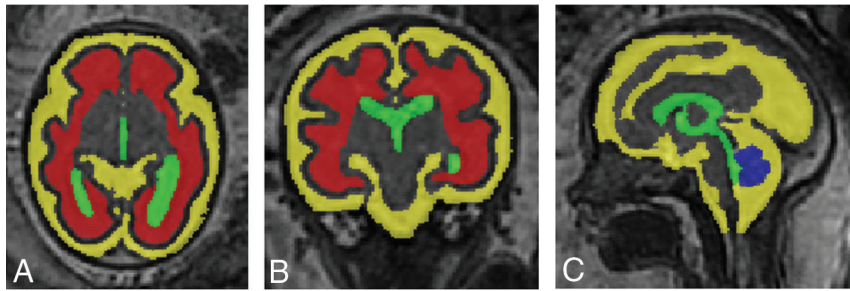


**FIG 1.** T2-weighted images in the axial (A), coronal (B), and sagittal (C) planes illustrating automated segmentations of the extra-axial space (yellow), white matter (red), ventricular system (green), and cerebellum (blue).

**General characteristics of the congenital diaphragmatic hernia group**

| General Characteristics                                     |                                |
|---|--------------------------------|
| Left/right/bilateral o/e TFLV at first MR imaging           | 28 (66.7%)/12 (28.6%)/2 (4.8%) |
| <15%  | 6 (14.2%)                      |
| 16%–25%   | 13 (31%)                       |
| 26%–45%   | 22 (52.4%)                     |
| >45%  | 1 (2.4%)                       |
| Liver herniation  | 40 (95.2%)                     |
| Liver/thorax ratio  | 30.13 (9.67)                   |
| Fetal position at MR imaging 1 (cephalic/breech/transverse) | 28 (67%)/13 (31%)/1 (2%)       |
| Fetal position at MR imaging 2 (cephalic/breech/transverse) | 37 (88%)/5 (12%) / 0           |
| GA at MR imaging 1 (mean)                                   | 28.0 (SD, 2.1)                 |
| GA at MR imaging 2 (mean)                                   | 33.2 (SD, 1.3)                 |
| Individual interval   | 4.83 (1.85)                    |
| Fetal endoluminal tracheal occlusion                        | 40 (95%)                       |

**Note:**—o/e indicates observed over expected ratio.

ventricle, and aqueduct), the cavum septi pellucidi and cavum vergae, extra-axial space, and cerebellum with manual correction when necessary (D.E. supervised by M.A.). A deep learning algorithm for the automatic segmentation of white matter, the ventricular system, and cerebellum was used for the first volumes that were processed.<sup>24</sup> As the number of volumes segmented for the extra-axial space increased, we trained a new deep learning-based segmentation algorithm<sup>25</sup> based on a partially supervised learning method that automatically segments white matter, the ventricular system, the cerebellum, and the extra-axial space. These segmentations were used for volumetric analysis when the quality of the SRR volume allowed further analysis (determined by D.E. and supervised by M.A. and L.F.) (Fig 1).

In all cases in which the fetus underwent fetal endotracheal occlusion (FETO), the date was noted and the time interval between the operation and second MR imaging was documented. The severity of pulmonary hypoplasia in fetuses with CDH was assessed on MR imaging by measuring the right, left, and total fetal lung volume (TFLV), the fetal body volume, liver position, intrathoracic liver volume, and thoracic volume, again measured manually (D.E. supervised by M.A.). From those, we calculated the observed over expected ratio TFLV ratio<sup>26</sup> and the liver-to-thoracic volume ratio.<sup>27</sup> The latter ratios provide biometric measurements in the index case that are independent of GA and/or fetal weight.

**Statistics**

Data were analyzed with Analyze-it (Analyze-it for Microsoft Excel 4.81.4; <https://analyze-it.com/>). Data were checked for normality using the Shapiro-Wilk test for normality. All data are expressed as mean (SD) or median (interquartile range), depending on normality; subclassifications were illustrated as number (percentage). Regression analysis of the different variables in healthy fetuses allowed calculation of normal ranges in correlation with GA for each parameter.

This allowed us to calculate an expected value for each observation in the CDH population. Differences between the CDH population at the first and the second time points and the controls were studied with the Wilcoxon-Mann-Whitney test, using the observed/expected ratios based on the reference cohort. To analyze the evolution with time, we performed a Wilcoxon hypothesis test on the difference in the observed/expected ratio between both time points. Correlations were assessed using the Pearson correlation coefficient, and the Bonferroni correction for multiple comparisons was performed.

**Ethics Approval**

This study was approved by the Ethics Committee of the University Hospitals Leuven (S56786).

**RESULTS**

**Study Population**

Twenty-eight fetuses had left, 12 had right, and 2 had bilateral CDH (*n* = 42; Table). The mean GA at the first MR imaging was 28.0 (SD, 2.1) weeks, and at the second, it was 33.2 (SD, 1.3) weeks. The mean difference between the 2 measurements was 4.8 (SD, 1.9) weeks. FETO was performed in 40 fetuses (95%) with a mean GA at FETO of 29.3 (SD, 1.5) weeks. The mean number of days between FETO and the second MR imaging was 26.45 (SD, 11.76). Balloon removal was performed at a mean GA of 33.5 (SD, 1.1) weeks. The mean GA in controls was 30.7 (SD, 4.2) weeks. SRR for volumetric analysis was possible in 25 (60%) fetuses at the first time point and in 23 (55%) at the second time point. Further details of success rates for volumetric measurements at the first and second time points and the number of available measures from paired data are shown in the Online Supplemental Data. In controls, 52 (93%) reconstructions were possible.

**Measurement at the First Time Point**

The fetal brain and skull biometry were not different between fetuses with CDH and those without. The extra-axial space and atrial width in fetuses with CDH were within the normal range, except for 1 fetus having mild ventriculomegaly (11 mm). The total brain cortical grading for fetuses with CDH was significantly lower than in controls (*P* < .003) (Online Supplemental Data). When we compared the brain grading of each hemisphere, the difference was present on both sides (both *P* < .003). The opercularization was delayed on the left side (*P* = .011), but not on the

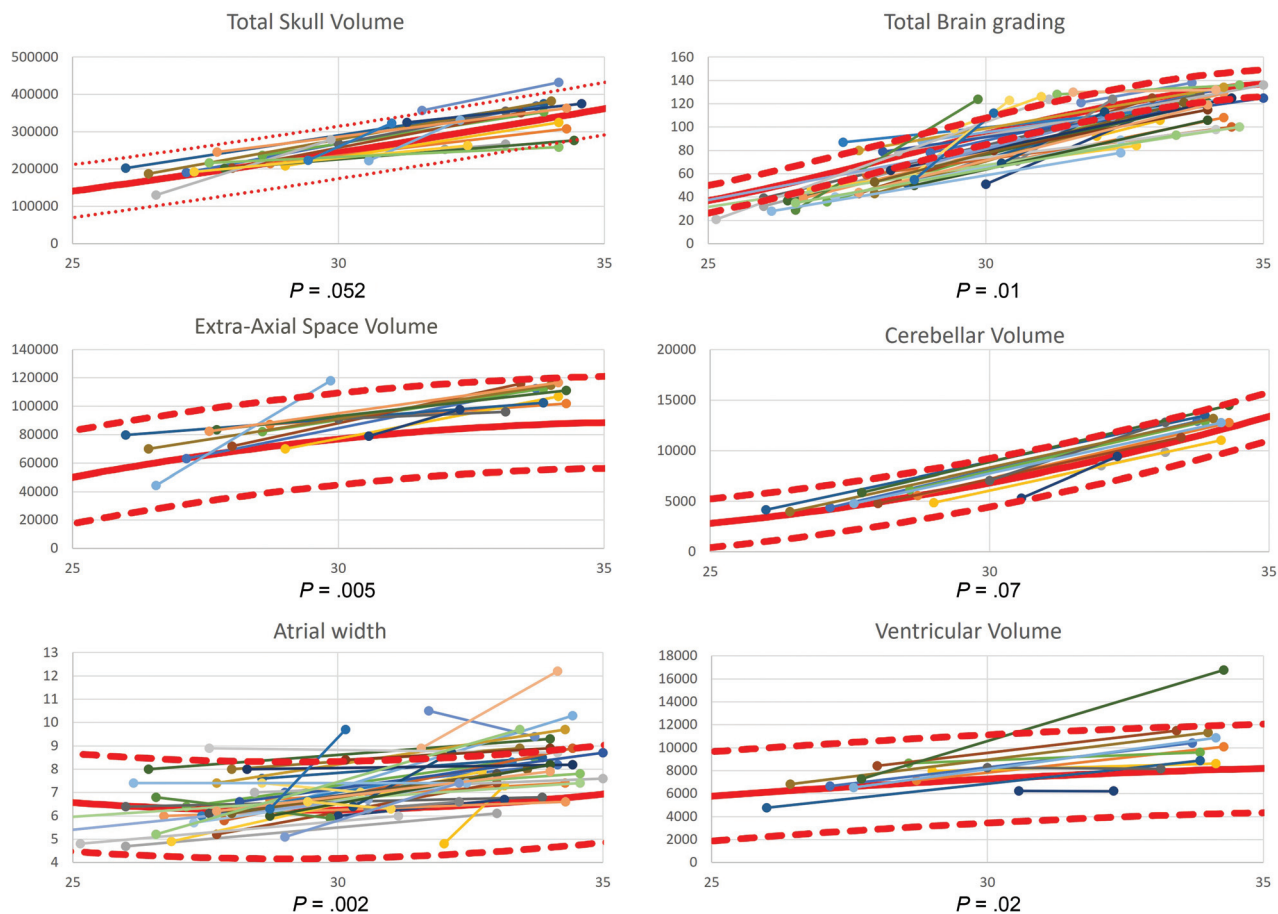


**FIG 2.** Graphs demonstrating the paired observations of the total skull volume, total brain grading, extra-axial space volume, cerebellar volume, atrial width, and ventricular volume. The provided  $P$  value is the significance level of the Wilcoxon-Mann-Whitney test comparing the observations at the second time point in fetuses with congenital diaphragmatic hernia with that in healthy controls. The mean values of the control populations (full red line) with the 95% confidence intervals (dashed red line) are also shown.

right ( $P = .057$ ). There was a reduced depth of the parieto-occipital fissure ( $P < .003$  on the right and  $P = .003$  on the left) and cingulate fissure (left and right,  $P < .003$ ), but the depth of the calcarine fissure was normal on both sides ( $P > .05$ ) compared with controls. The Sylvian fissure was just significantly deeper only on the right ( $P = .042$ ), but not on the left ( $P = .055$ ) in fetuses with CDH. The insular depth in fetuses with CDH was within the normal range ( $P > .05$ ). There was no difference in volume of the total skull, extra-axial space, ventricular system, white matter, or cerebellum between fetuses with CDH and healthy controls (Online Supplemental Data).

#### Measurement and Change at the Second Time Point

At the second time point, most measurements were within the normal range, except for the atrial width ( $P < .003$ ), the ventricular volume ( $P = .024$ ), and the extra-axial space volume ( $P = .005$ ), which were larger than normal. The total brain cortical grading was lower than normal ( $P = .011$ ) on both sides ( $P = .019$  and  $P = .035$ ), and the opercularization was within the normal range ( $P > .05$ ) (Fig 2). The Sylvian fissure depth was deeper (both  $P < .003$ ), but all other fissures were comparable with those in controls. Compared with findings on the initial scans, the atrial width increased further, and the brain fissures that were initially

less deep measured within the normal range. The depth of the Sylvian fissure, which was normal earlier, became abnormally deeper; also, the left-brain hemisphere cortical grading score was abnormal, but significantly less so than at the first time point. Although the difference in brain scoring between the CDH population and the controls was less at the second time point, this was not significantly different from the first time point (Online Supplemental Data).

#### Correlation with Severity Indicators of Lung Hypoplasia

No correlation was found at either time point between the liver-to-thorax ratio or the observed over expected ratio TFLV on one side or the total brain grading, skull and brain fronto-occipital diameter, atrial width, ventricular volume or extra-axial space volume, cerebellar volume, or total intracranial volume on the other side. No significant difference was found in the variables mentioned above when comparing fetuses with left and right CDH.

#### DISCUSSION

Danzer et al<sup>18</sup> reported a lower total maturation score in infants with CDH after birth.<sup>6</sup> Along the same lines, Lucignani et al<sup>28</sup> reported reduced cortical maturation in extended brain areas of

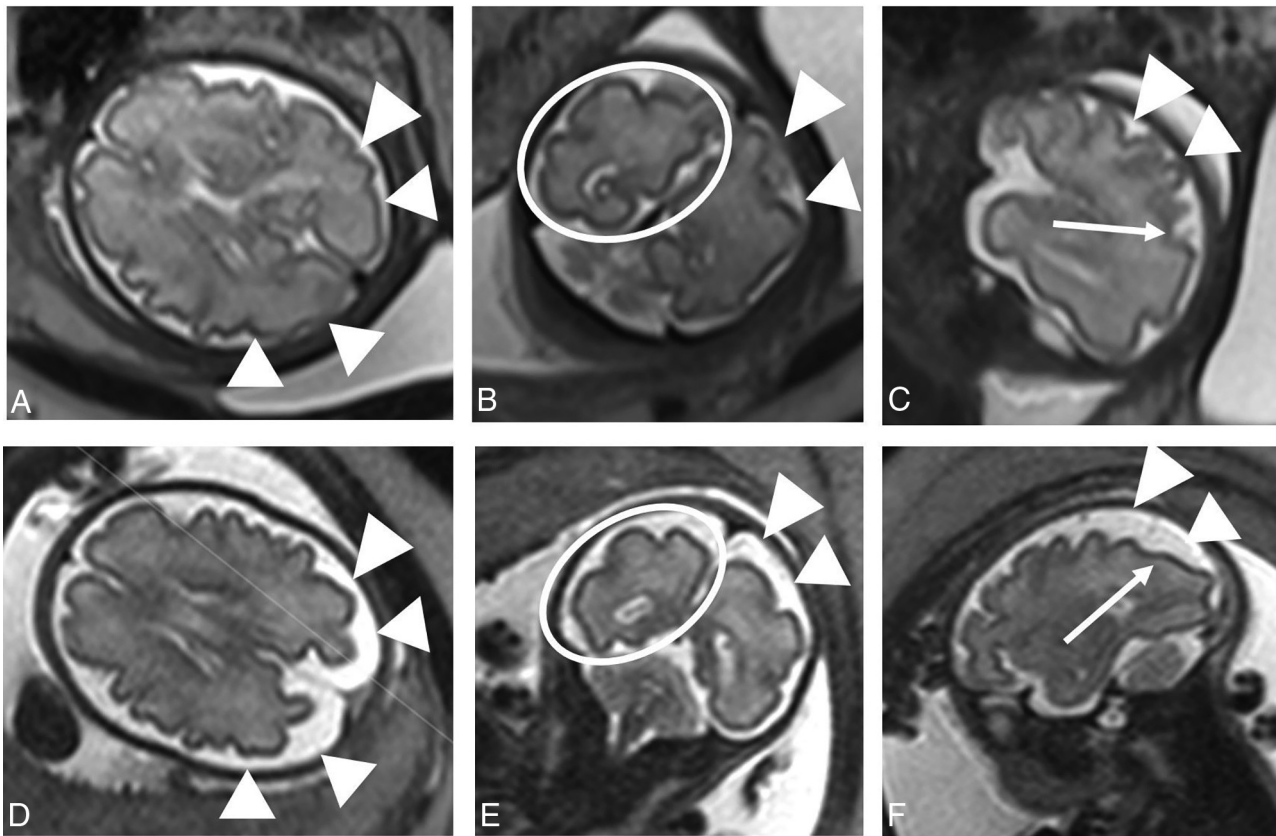


**FIG 3.** Three orthogonal T2-weighted spin-echo images in a healthy fetus (A–C) and a fetus with a left-sided diaphragmatic hernia (D–F), both at a GA of 30 weeks 4 days. In the axial plane (A and D), the enlarged pericerebral space is evident (arrowheads). The difference in gyrication is most evident in the parietal area and best seen in the coronal plane (circle in B and E) and to a lesser extent in the sagittal plane (arrows in C and F). The enlarged pericerebral space in the coronal and sagittal planes is marked with arrowheads.

neonates with CDH compared with healthy controls. In earlier prenatal studies, fetuses with CDH had brain sulcation scores that are indicators of prenatal brain maturation, within the normal range between 20 and 37 weeks.<sup>12,29</sup> One study on infants who had both pre- and postnatal imaging reported signs of brain injury (eg, hemorrhage, white matter injury. . .) on postnatal but not on prenatal MR imaging. In that study, the injury score correlated with the degree of pulmonary hypoplasia without an indication of delayed sulcation in those fetuses.<sup>29</sup>

Conversely, our study demonstrates that fetuses with CDH have indications of atypical brain development, ie, with a significant delay at 28 and 33 weeks of gestation (Fig 3). By 33 weeks, the quantitative scores were in the normal range. However, quantitative scoring was performed on primary and not on secondary sulci, limiting the detection of subtle folding abnormalities.<sup>30</sup> The qualitative scoring system we used allows a thorough scoring of brain sulcation throughout a wide GA range, because it evaluates the primary formation as well as the presence of secondary and tertiary sulcation.<sup>20</sup> We were not able to compare our morphologic findings with the postnatal clinical neurobehavioral assessment. In infants with CDH, 9% (4%–14%) have abnormal opercularization, which translates later into language and speech abnormalities.<sup>7</sup> In our study, grading of the operculum was significantly lower at the first time point and at the second time point, though only left-sided. It remains unclear whether the

abnormalities we found are related to any of the reported functional consequences observed in infants with CDH or other abnormalities. In earlier studies, scores using the same system correlated well with the Neonatal Behavioral Assessment Scale,<sup>31</sup> though this correlation was in fetuses with isolated nonsevere ventriculomegaly or late-onset growth restriction.<sup>14,22</sup> The functional impact of our observations in fetuses with CDH remains to be elucidated. Moreover, one must take into account that any abnormality observed postnatally may as well have been acquired after birth.

Irrespective of the functional impact, the cause of atypical brain folding that we observed in fetuses remains unclear. One factor may be a degree of hemodynamic dysfunction. We have previously reported a decline in the systolic velocity of the MCA peak, hence in brain perfusion in fetuses with CDH.<sup>14,32</sup> One may recognize similarities to circulatory disturbances in fetuses with congenital heart defects, which coincide with signs of abnormal brain development. In hypoplastic left heart syndrome, a lower blood flow velocity has been associated with lower brain volume.<sup>33,34</sup> Furthermore, fetuses with this and other congenital heart defects had delayed brain maturation in the late second and early third trimesters, and again, this has been linked to abnormal hemodynamics and oxygen delivery.<sup>35</sup> Lucignani et al<sup>28</sup> also used this theory to explain their recent findings of altered cortical maturation in neonates with CDH.

The significant increase in the volume of all fluid compartments at 33 weeks' gestation in CDH that we observed (Fig 3) is in line with work of Radhakrishnan et al.<sup>12</sup> Because fetuses had normal biometry of the cerebral hemispheres and lacked major parenchymal abnormalities, the authors questioned the clinical relevance of these findings. Recently, the importance was shown of a diagnostic algorithm that helps to discriminate fetuses with enlargement of the extra-axial space with self-limiting delays from those at risk of a persistent delay.<sup>36</sup> Abnormal intracranial fluid volumes have been previously explained by a change in cardiac output in CDH caused by herniation of abdominal structures in turn leading to mild or moderate cardiac hypoplasia in left-sided CDH or cardiac compression, compromising venous return.<sup>29,37</sup> This may, in turn, cause venous congestion and lead to decreased CSF resorption<sup>38</sup> and an overall increase of intracranial fluid. It may be useful to assess cardiac function and hemodynamics in more detail in fetuses with CDH to study whether there is a link with brain development.

We are the first to document in utero brain development in fetuses with CDH using a structured brain evaluation. For this evaluation, we used fetal brain MR imaging because this allows a standardized and reproducible in-depth analysis, as illustrated by other studies.<sup>21,22</sup> Our analysis was not limited to a qualitative, ie subjective, analysis of the brain maturation but also included a quantitative scoring method.<sup>20,21</sup> Furthermore, we used a sophisticated segmentation technique<sup>25</sup> based on high-resolution motion-corrected 3D volumes.<sup>23</sup> Because all examinations were performed around the time the fetus was assessed for FETO, the GA range in our population is also relatively narrow and at a point at which cortical maturation has already progressed far enough to illustrate subtle differences. Additionally, this range means that the information from our study is from a relevant time point in pregnancy with respect to fetal therapy.

Nevertheless, we acknowledge several limitations. First, its retrospective design may result in selection bias because we included only fetuses with >1 good-quality MR imaging examination and in whom we were able to create a good-quality 3D SRR reconstruction. Second, because we are a fetal surgery center, the group of fetuses with severe hypoplasia is over-represented, and most fetuses (40/42, 95%) underwent FETO between MR imaging examinations. Hence, there may have been an effect of fetal surgery on the second MR imaging because FETO changes the natural history.<sup>9-11,39</sup> Third, we have no standardized postnatal follow-up information on these cases because many patients do not deliver at our center.

Our results mandate further investigation into the sulcation pattern beyond 34 weeks in fetuses with CDH, including quantitative methods, eg, analysis of cortical folding patterns,<sup>40</sup> cortical thickness, and the local gyrification index,<sup>28</sup> as well as earlier in fetuses not undergoing fetal therapy.

## CONCLUSIONS

We report delayed brain development in fetuses with CDH around 28 weeks, which becomes less prominent at 33 weeks. With the advent of fetal surgery,<sup>9,10</sup> this might become more relevant because it suggests altered brain development in utero in these fetuses. Of note, there was no correlation between brain

development and the severity of lung hypoplasia in this highly selected group. We also observed an increase in extra-axial space and also in ventricular volume in the third trimester.

Disclosure forms provided by the authors are available with the full text and PDF of this article at [www.ajnr.org](http://www.ajnr.org).

## REFERENCES

- Leeuwen L, Fitzgerald DA. **Congenital diaphragmatic hernia.** *J Paediatr Child Health* 2014;50:667–73 [CrossRef Medline](#)
- Montalva L, Raffler G, Riccio A, et al. **Neurodevelopmental impairment in children with congenital diaphragmatic hernia: not an uncommon complication for survivors.** *J Pediatr Surg* 2020;55:625–34 [CrossRef Medline](#)
- Antiel RM, Lin N, Licht DJ, et al. **Growth trajectory and neurodevelopmental outcome in infants with congenital diaphragmatic hernia.** *J Pediatr Surg* 2017;52:1944–48 [CrossRef Medline](#)
- Partridge EA, Bridge C, Donaher JG, et al. **Incidence and factors associated with sensorineural and conductive hearing loss among survivors of congenital diaphragmatic hernia.** *J Pediatr Surg* 2014;49:890–94; discussion 894 [CrossRef Medline](#)
- Danzer E, Gerdes M, D'Agostino JA, et al. **Neurodevelopmental outcome at one year of age in congenital diaphragmatic hernia infants not treated with extracorporeal membrane oxygenation.** *J Pediatr Surg* 2015;50:898–903 [CrossRef Medline](#)
- Bevilacqua F, Morini F, Zaccara A, et al. **Neurodevelopmental outcome in congenital diaphragmatic hernia survivors: role of ventilatory time.** *J Pediatr Surg* 2015;50:394–98 [CrossRef Medline](#)
- Van der Veeken L, Vergote S, Kunpalin Y, et al. **Neurodevelopmental outcomes in children with isolated congenital diaphragmatic hernia: a systematic review and meta-analysis.** *Prenat Diagn* 2022;42:318–29 [CrossRef Medline](#)
- Danzer E, Zarnow D, Gerdes M, et al. **Abnormal brain development and maturation on magnetic resonance imaging in survivors of severe congenital diaphragmatic hernia.** *J Pediatr Surg* 2012;47:453–61 [CrossRef Medline](#)
- Deprest JA, Benachi A, Gratacos E, et al; TOTAL Trial for Moderate Hypoplasia Investigators. **Randomized trial of fetal surgery for moderate left diaphragmatic hernia.** *N Engl J Med* 2021;385:119–29 [CrossRef Medline](#)
- Deprest JA, Nicolaides KH, Benachi A, et al; TOTAL Trial for Severe Hypoplasia Investigators. **Randomized trial of fetal surgery for severe left diaphragmatic hernia.** *N Engl J Med* 2021;385:107–18 [CrossRef Medline](#)
- Russo FM, Cordier AG, Basurto D, et al. **Fetal endoscopic tracheal occlusion reverses the natural history of right-sided congenital diaphragmatic hernia: European multicenter experience.** *Ultrasound Obstet Gynecol* 2021;57:378–85 [CrossRef Medline](#)
- Radhakrishnan R, Merhar SL, Burns P, et al. **Fetal brain morphometry on prenatal magnetic resonance imaging in congenital diaphragmatic hernia.** *Pediatr Radiol* 2019;49:217–23 [CrossRef Medline](#)
- Tracy S, Estroff J, Valim C, et al. **Abnormal neuroimaging and neurodevelopmental findings in a cohort of antenatally diagnosed congenital diaphragmatic hernia survivors.** *J Pediatr Surg* 2010;45:958–65 [CrossRef Medline](#)
- Van der Veeken L, Russo FM, Litwinska E, et al. **Prenatal cerebellar growth is altered in congenital diaphragmatic hernia on ultrasound.** *Prenat Diagn* 2022;42:330–37 [CrossRef Medline](#)
- Srisupundit K, Brady PD, Devriendt K, et al. **Targeted array comparative genomic hybridisation (array CGH) identifies genomic imbalances associated with isolated congenital diaphragmatic hernia (CDH).** *Prenat Diagn* 2010;30:1198–206 [CrossRef Medline](#)
- Kyriakopoulou V, Vatanserver D, Davidson A, et al. **Normative biometry of the fetal brain using magnetic resonance imaging.** *Brain Struct Funct* 2017;222:2295–307 [CrossRef Medline](#)
- Garel C. **Fetal cerebral biometry: normal parenchymal findings and ventricular size.** *Eur Radiol* 2005;15:809–13 [CrossRef Medline](#)

18. Saleem SN. **Fetal MRI: an approach to practice—a review.** *J Adv Res* 2014;5:507–23 [CrossRef Medline](#)
19. Aertsen M, Dymarkowski S, Vander Mijnsbrugge W, et al. **Anatomical and diffusion-weighted imaging abnormalities of third-trimester fetal brain in cytomegalovirus-infected fetuses.** *Ultrasound Obstet Gynecol* 2022;60:68–75 [CrossRef Medline](#)
20. Pistorius LR, Stoutenbeek P, Groenendaal F, et al. **Grade and symmetry of normal fetal cortical development: a longitudinal two- and three-dimensional ultrasound study.** *Ultrasound Obstet Gynecol* 2010;36:700–08 [CrossRef Medline](#)
21. Egaña-Ugrinovic G, Sanz-Cortes M, Figueras F, et al. **Differences in cortical development assessed by fetal MRI in late-onset intrauterine growth restriction.** *Am J Obstet Gynecol* 2013;209:126e1–8 [CrossRef Medline](#)
22. Hahner N, Benkarim OM, Aertsen M, et al. **Global and regional changes in cortical development assessed by MRI in fetuses with isolated nonsevere ventriculomegaly correlate with neonatal neurobehavior.** *AJNR Am J Neuroradiol* 2019;40:1567–74 [CrossRef Medline](#)
23. Ebner M, Wang GT, Li WQ, et al. **An automated framework for localization, segmentation and super-resolution reconstruction of fetal brain MRI.** *Neuroimage* 2020;206:116324 [CrossRef Medline](#)
24. Fidon L, Aertsen M, Mufti N, et al. **Distributionally robust segmentation of abnormal fetal brain 3D MRI: uncertainty for safe utilization of machine learning in medical imaging, and perinatal imaging, placental and preterm image analysis.** In: *Proceedings of the 3rd International Workshop, UNSURE 2021, and 6th International Workshop, PIPPI 2021, Held in Conjunction with MICCAI 2021, Strasbourg, France, October 1, 2021*
25. Fidon L, Aertsen M, Emam D, et al. **Label-set loss functions for partial supervision: application to fetal brain 3D MRI parcellation.** *arXiv* 2021:2107.03846 <https://arxiv.org/abs/2107.03846>. Accessed August 1, 2021
26. Cannie MM, Jani JC, Van Kerkhove F, et al. **Fetal body volume at MR imaging to quantify total fetal lung volume: normal ranges.** *Radiology* 2008;247:197–203 [CrossRef Medline](#)
27. Cannie M, Jani J, Chaffiotte C, et al. **Quantification of intrathoracic liver herniation by magnetic resonance imaging and prediction of postnatal survival in fetuses with congenital diaphragmatic hernia.** *Ultrasound Obstet Gynecol* 2008;32:627–32 [CrossRef Medline](#)
28. Lucignani M, Longo D, Fontana E, et al. **Morphometric analysis of brain in newborn with congenital diaphragmatic hernia.** *Brain Sci* 2021;11:455 [CrossRef Medline](#)
29. Radhakrishnan R, Merhar SL, Su W, et al. **Prenatal factors associated with postnatal brain injury in infants with congenital diaphragmatic hernia.** *AJNR Am J Neuroradiol* 2018;39:558–62 [CrossRef Medline](#)
30. Garel C, Elmaleh M, Chantrel E, et al. **Fetal MRI: normal gestational landmarks for cerebral biometry, gyration and myelination.** *Childs Nerv Syst* 2003;19:422–25 [CrossRef Medline](#)
31. Brazelton TB, Nugent JK. *Neonatal Behavioral Assessment Scale.* Cambridge University Press; 1995:200
32. Van Mieghem T, Sandaite I, Michielsens K, et al. **Fetal cerebral blood flow velocities in congenital diaphragmatic hernia.** *Ultrasound Obstet Gynecol* 2010;36:452–57 [CrossRef Medline](#)
33. Kaltman JR, Di H, Tian Z, et al. **Impact of congenital heart disease on cerebrovascular blood flow dynamics in the fetus.** *Ultrasound Obstet Gynecol* 2005;25:32–36 [CrossRef Medline](#)
34. Pearce W. **Hypoxic regulation of the fetal cerebral circulation.** *J Appl Physiol (1985)* 2006;100:731–38 [CrossRef Medline](#)
35. Jaimes C, Rofeberg V, Stopp C, et al. **Association of isolated congenital heart disease with fetal brain maturation.** *AJNR Am J Neuroradiol* 2020;41:1525–31 [CrossRef Medline](#)
36. Maruccia F, Gomáriz L, Rosas K, et al. **Neurodevelopmental profile in children with benign external hydrocephalus syndrome: a pilot cohort study.** *Childs Nerv Syst* 2021;37:2799–806 [CrossRef Medline](#)
37. Vogel M, McElhinney DB, Marcus E, et al. **Significance and outcome of left heart hypoplasia in fetal congenital diaphragmatic hernia.** *Ultrasound Obstet Gynecol* 2010;35:310–17 [CrossRef Medline](#)
38. Miyajima M, Arai H. **Evaluation of the production and absorption of cerebrospinal fluid.** *Neurol Med Chir (Tokyo)* 2015;55:647–56 [CrossRef Medline](#)
39. Basurto D, Russo FM, Van der Veecken L, et al. **Prenatal diagnosis and management of congenital diaphragmatic hernia.** *Best Pract Res Clin Obstet Gynaecol* 2019;58:93–106 [CrossRef Medline](#)
40. Orasanu E, Melbourne A, Cardoso MJ, et al. **Cortical folding of the preterm brain: a longitudinal analysis of extremely preterm born neonates using spectral matching.** *Brain Behav* 2016;6:e00488 [CrossRef Medline](#)